BOX COMPRESSION ANALYSIS OF WORLD-WIDE DATA SPANNING 46 YEARS

Thomas J. Urbanik
Research Engineer
USDA Forest Service
Forest Products Laboratory[1]
One Gifford Pinchot Drive
Madison, WI 53726

and

Benjamin Frank
Manager
Materials Optimization and Development
Packaging Corporation of America
Mundelein, IL 60060

(Received April 2005)

ABSTRACT

The state of the art among most industry citations of box compression estimation is the equation by McKee developed in 1963. Because of limitations in computing tools at the time the McKee equation was developed, the equation is a simplification, with many constraints, of a more general relationship. By applying the results of sophisticated finite element modeling, in this current study we derive a more general box compression formula that preserves the underlying theory of the McKee equation but removes the constraints. This formula is solvable with modern spreadsheet software, and we present an implementation method and example outputs as we relax or impose the various constraints. We analyze data obtained from multiple literature sources containing the traditional McKee equation inputs. We quantify the disparity between the McKee equation and the various sources of data and present an improved model for single-wall box-compression strength. The model attaches physical meaning to what were previously only fitting parameters, and it can serve as a tool for additional explorations in box optimization.

Keywords: Box compression, strength, model, bending stiffness, ECT, BCT, buckling.

INTRODUCTION

Corrugated fiberboard is a primary material in the shipping, distribution, and storage of almost every product. Boxes made from corrugated board provide temporary protection from compression forces for products in transit or stacked in warehouses. In this environment, top-to-bottom box compression strength is an important performance criterion that may even be specified in the negotiation of price.

Ever since the broadening of motor freight and rail carrier classifications in 1936 to include corrugated fiberboard shipping containers, manufacturers have sought predictive strength models for corrugated boxes. Researchers have attempted to generate predictive equations that would reliably estimate box compression strength without requiring the actual production and testing of every box. At the USDA Forest Products Laboratory, Madison, Wisconsin, initial scientific analysis of boxes predates World War II. Kellicutt and Landt (1951) summarized much of this work with basic design principles

[1] The Forest Products Laboratory is maintained in cooperation with the University of Wisconsin. This article was written and prepared by U.S. Government employees on official time, and it is therefore in the public domain and not subject to copyright.

in terms of correlations between material compression strength and panel buckling strength. In this study, we expand upon those same principles.

McKee et al. (1963) published what has become the industry's seminal article in this area, including detailed citations of the literature that preceded their analysis. Their work resulted in an equation to predict single-wall (SW) box-compression strength P, commonly called simply the "McKee equation," of the form

$$P = aP_{\mathrm{m}}^{b}(\sqrt{D_{\mathrm{x}}D_{\mathrm{y}}})^{1-b}Z^{2b-1} \qquad (1)$$

where P_{m} is the edge-crush value of the combined board, D_{x} and D_{y} are the flexural stiffness values for the combined board in each direction, and Z is the perimeter of the box to be modeled. As we shall discuss, this functional form is a simplification, with many constraints, of a more general relationship. Similar functional forms were found by Buchanan et al. (1964) and Shick and Chari (1965) to work for double-wall (DW) containers as well. Wolf (1972), Batelka and Smith (1993), and Challas et al. (1994) found it important to include additional terms to account for the box geometry, though the various approaches that include geometry explicitly do not agree.

Using Eq. (1), McKee et al. (1963) reported the average difference in magnitude between predicted and actual compression strength of their data set as 6.1%, with 97% of their data within ±15% of the estimated value and a maximum difference of 17.1%. Subsequent literature reported even better accuracy for specific data sets with geometry effects included. However, the goal of developing a predictive model should not be an equation that describes a limited data set exceptionally well but rather an equation with good inter-laboratory precision and accuracy—one that can adequately address all the available data.

The round-robin analysis of compression data on actual containers by Miles (1966) provides an objective quantification of how accurate any model could be expected to be. Eleven laboratories tested empty regular slotted containers of a single material grade and size. The simplest model of all the data would make P equal to the overall average strength. Given that model parameters are generated with real world data, we cannot expect any model to do better than the variability in testing of the input parameters. However, the difference between experimental variability and modeling variability is a real cost associated with box production, resulting in boxes that may be over-designed to compensate for a lack of model precision. Improving the accuracy of our models would remove some of this extra cost from the manufacturing process.

The various studies estimating box compressive strength do not all report the same values for a or b in their fits to Eq. (1), though they all typically report their values to three or more "significant" figures. They also do not report the statistical range on these values, which is of interest given that all the values were arrived at through curve fitting. As an example, simply by reading the articles, we do not know if McKee's value $b = 0.746$ is equivalent to the value 0.75 used by Wolf (1972), 0.724 used by Shick and Chari (1965), or 0.778 found by Buchanan et al. (1964). More recent literature might lead us to conclude that ~0.75 is a reasonable value for the exponent b, while 2–3 is a reasonable value for a, independent of the construction of the corrugated container. While in practice these simplifications are often implemented at some loss of accuracy in estimation quality, it is not clear that they are legitimate for each data set individually or for the entire mass of data available in the literature. Furthermore, increasing a by 50% in a given equation would lead to a 50% increase in predicted box compression. Clearly this is not realistic for a given set of data.

It is also important to note that in many analyses that have followed McKee's analysis, the original parameters (a and b) of the McKee equation are assumed in one form or another. The data sets themselves are fit only insofar as changes are made to the initial form, typically by incorporating the impact of box dimensions. This approach raises questions about the validity

of the resulting functional forms, given that all the parameters were not allowed to change independently during the minimization of the error term in the fitting process.

Aside from production variables, at least 17 elastic constants appear to be applicable to corrugated fiberboard. Libove and Hubka (1951) identified 12 constants, of which three were checked experimentally, appropriate to general symmetrical corrugated-core sandwich plates. Asymmetric plates need an additional five coupling constants. In this report, our theory includes four of the constants in the form of D_x, D_y, $\hat{c}$, and ν, and as we will show, most individual data sets can be characterized working only with D_x and D_y. With broadened data, Kellicutt and Landt (1951) and Kawabata (1997) advocated empirical flute-adjustment factors. However, with the exception of our parameter τ, we reserve such adjustments and a rationale for reducing 17 elastic constants to an effective four constants for future work. We shall also cite a background nonlinear material theory, but limit this report to a linear material theory.

OBJECTIVE

Working with dimensionless expressions instead of the elastic constants helped Urbanik and Saliklis (2003) to understand the developed models, even though such expressions are not typically encountered among box designers. The objective of this report is to apply the results of previous work (Urbanik and Saliklis 2003) to analyze all known available box compression strength data. We compile and analyze 19 data sources[1] currently available, explain some discrepancies among estimation formulas found in the literature, and provide a deeper understanding of the factors that influence estimation of box compression. The assumptions made throughout are that container performance is fixed by the physics of the boxes tested, and the purpose of testing and estimation is to arrive at fundamental physics to best understand and predict failure mechanisms. With that in mind, we also uncover several areas for additional research and expansion on current knowledge. This work is necessary if the corrugated container industry hopes to understand its product well and achieve materials savings and economy by reducing product variation.

LINEAR MODEL

Advancements in the understanding of paper material have allowed researchers to investigate the effects of material properties and geometry on corrugated fiberboard strength that were not considered in the McKee formula. In particular, comparisons by Urbanik and Saliklis (2003) between finite element predictions of plate buckling strength and fitted formulas enabled researchers to numerically investigate a broad-based strength response of simulated box panels economically.

The two-part formula given by Urbanik and Saliklis (2003) characterizing the postbuckling strength of box panels can be expressed more simply as

$$\frac{P_f}{P_y} = \alpha \left(\frac{P_{cr}}{P_y} \right)^{u\eta} \tag{2}$$

Input $u = 1$ characterizes elastic buckling appropriate when the slenderness ratio $U > 1$, or, in other words, when the total load the plate can support exceeds the critical buckling load, and $u = 0$ characterizes inelastic buckling when $U \leq 1$. Only elastic buckling was considered by McKee et al. (1963) in the development of Eq. (1).

Complexities in calculation led McKee et al. (1963) to simplify the fundamental Eq. (2) to reach Eq. (1). To remove these limiting assumptions, we start with Eq. (2) in its most general-

[1] Data analyzed in this study were taken from Angell and Paslay (1959), Batelka and Smith (1993), Bormett et al. (1981), Brodeur et al. (1997), Buchanan et al. (1964), Challas et al. (1994), Fahey and Bormett (1982), Gartaganis (1975), Hahn et al. (1992), Hartikainen (1989), IPC (1967), Koning and Moody (1969), Koning and Godshall (1975), Little (1943), McKee et al. (1963), Schrampfer et al. (1987), and Shick and Chari (1965). We also used unpublished data from P. McKinlay and B. Frank (Materials Testing Laboratory, Packaging Corporation of America).

ized form and follow the procedures of Urbanik and Saliklis (2003).

$$\frac{P_f}{P_y} = \alpha\theta_0^{u\eta}\hat{\sigma}_a^{u\eta} \tag{3}$$

Equation (3) is applicable to either a linear or nonlinear material law. Corrugated fiberboard is inherently a nonlinear material, with curvature in its load-strain relationship. Furthermore, evidence from sophisticated modeling seems to favor a nonlinear input. However, to fully understand nonlinear material modeling, we must thoroughly understand the linear material response. Thus, in this study we investigate the response involving only a linear material law and incorporate the rule $\hat{\sigma}_a = CS\phi^{\tau}$ to obtain

$$\frac{P_f}{P_y} = \alpha\theta_0^{u\eta}(CS\phi^{\tau})^{u\eta} \tag{4}$$

Another implicit assumption in the McKee formula is the form of the critical load $\overline{P_{cr}}$ appropriate for an infinitely long plate, neglecting twisting mechanics. By replacing the plate stiffness S in Eq. (4) with equivalent physical properties, we are able to treat the general case of P_{cr} expressed in relation to $\overline{P_{cr}}$

$$\frac{P_f}{P_y} = \alpha\theta_0^{u\eta}\left(C\frac{12\sqrt{D_xD_y}}{\theta_0 P_y l^2}\phi^{\tau}\right)^{u\eta} = \alpha\left(\frac{3C\phi^{\tau}}{\pi^2}\right)^{u\eta}\left(\frac{\overline{P_{cr}}}{P_y}\right)^{u\eta} \tag{5}$$

Equation (5) and input $\overline{P_{cr}}$ are written with box panel dimensions in mind—with either length l or width w of the box input as the plate size. By calculating the compression for each panel and summing appropriately, we are able to avoid the assumption made by McKee that all boxes are square and that the perimeter Z should be used.

We also remove the McKee assumption that boxes must be relatively tall. By introducing parameter C into Eq. (5), we have accounted for buckling waviness in the direction of box depth and can deal with both tall and squatty boxes. The expression for C is to be evaluated for the simple support condition at the wave period given by $\chi = m\pi/2\phi$ and at the integer value of m that yields a minimum C.

$$C = \frac{\chi^2}{3(1-\nu^2)}\left(\left(\hat{c}+\frac{\pi^2}{4\chi^2}\right)^2 - \hat{c}^2 + 1\right) = \min_{m=1,2,3\ldots}\frac{\pi^2}{12(1-\nu^2)}\left(2\hat{c}+\frac{\phi^2}{m^2}+\frac{m^2}{\phi^2}\right) \tag{6}$$

The result of substituting the minimum C into Eq. (5) leads to

$$\frac{P_f}{P_y} = \alpha\left(\phi^{\tau}\frac{2\hat{c}+M}{4(1-\nu^2)}\right)^{u\eta}\left(\frac{\overline{P_{cr}}}{P_y}\right)^{u\eta}$$

$$M(m,\phi) = \min_{m=1,2,3\ldots}\left(\frac{\phi^2}{m^2}+\frac{m^2}{\phi^2}\right) \tag{7}$$

To obtain a form appearing as a more general expansion to Eq. (1), we can substitute expressions for $\overline{P_{cr}}$ and ϕ, transform constants as $\alpha = a(64\pi^2)^{b-1}$ and $\eta = 1 - b$, use $P_y = P_m$ and rearrange terms to get the following expressions for the cases of inelastic and elastic buckling:

For inelastic buckling,

$$P_l = P_f l = a16^{b-1}(4\pi^2)^{b-1}P_m l \qquad u=0 \tag{8}$$

For elastic buckling,

$$P_l = P_f l = a16^{b-1}P_m^b(\sqrt{D_xD_y})^{1-b}\, l^{2b-1}\left(\left(\frac{d}{l}\left(\frac{D_x}{D_y}\right)^{1/4}\right)^{\tau}\frac{2\hat{c}+M}{4(1-\nu^2)}\right)^{1-b} u = 1$$

Inelastic buckling typically occurs in box panels that are geometrically stiff (low l, low w, or high board thickness) relative to the material edgewise crush test (ECT) strength. If a box panel is observed to crush uniformly along its loading edge without significant bulging, it has probably failed by inelastic buckling. Conversely, if a panel noticeably bulges with crushing emanating from its corners, buckling is probably elastic. Computing the slenderness $U = \sqrt{P_y/P_{cr}}$ of the panel is a good predictor of what mechanism will occur.

Other material property inputs that relate to

TABLE 1. *Inputs to model and associated coding to impose or remove various constraints.*

With constraint			Without constraint		
Effect	Input	Code	Effect	Input	Code
Considers the box as square	$l = w = Z/4$	S	Models rectangular geometry	l, w	R
Neglects effect of box depth; assumes to be infinite[a]	$M = 2$	I	Models finite depth	$M(m, \phi)$	F
Considers only elastic buckling	$u = 1$	E	Models elastic and inelastic buckling	$u(U)$	EI
Neglects plate stiffening associated with effective aspect ratio	$\tau = 0$	—	Models aspect ratio stiffening	$\tau \neq 0$	—
Assumes that shear modulus associated with twisting conforms to St. Venant's principle	$\hat{c} = 1$	—	Models known shear modulus	$\hat{c}$	—
Neglects effect of plate twisting on Poisson's ratio	$\nu = 0$	—	Models known Poisson's ratio	ν	—

[a] The minimum of the function $M(m, \phi)$ occurs at real $m = \phi$. For an infinite depth plate this yields $M = 2$.

twisting through $\hat{c}$ and ν appear in Eqs. (7) and (8) but were not included in the McKee formula. Twisting of a corrugated panel is a difficult process to model, and a complete characterization must include within-plane shear stiffness and Poisson's ratios. Luo et al. (1995) suggested a pair of square-panel twisting tests for obtaining the requisite data. Angell and Paslay (1959), Buchanan et al. (1964), and McKinlay (1980)[2] reported partial data on the shear modulus. Complete twisting data do not appear to be present in the literature on box compression beyond the work of Luo et al. (1995). When twisting stiffness cannot be obtained, the inputs $\hat{c} = 1$ and $\nu = 0$ into Eqs. (7) and (8) are recommended.

Though Eqs. (4), (7), and (8) are equivalent, each form offers an advantage in looking at plate strength in terms of dimensionless variables or actual mechanical properties. Except for the introduction of empirical improvement τ, no nonmechanistic assumptions are made. Parameter τ accounts for the apparent predictability dependence on panel aspect ratio and can be understood as an adjustment to overall plate rigidity as affected by boundary conditions and geometry. It is interesting to impose the constraints from McKee et al. (1963) onto Eq. (8) individually (Table 1). Imposing all these constraints reduces Eq. (8) to $P_1 = P/4$ with P given by Eq. (1).

The logarithmic transformation of Eq. (7)

$$\log \frac{P_f}{P_y} = u\eta\left(\log \frac{2\hat{c} + M}{4(1 - \nu^2)} + \log \frac{\overline{P_{cr}}}{P_y}\right) + u\eta\tau\log\phi + \log\alpha \tag{9}$$

allows us to fit the available data with linear techniques. The best fit to the equation requires a minimization of the differences between the predicted panel strength ratio P_f/P_y and the experimental panel strength ratio P_f^*/P_y summed over all the available data.[3]

$$\min\left(\sum\left(\log \frac{P_{fl}}{P_y} - \log \frac{P_{fl}^*}{P_y}\right)^2 + \sum\left(\log \frac{P_{fw}}{P_y} - \log \frac{P_{fw}^*}{P_y}\right)^2\right) \tag{10}$$

Depending on box geometry, the strength of the side panel P_{fl} might differ from the strength of the end panel P_{fw}. Experimental (actual) panel strength is not known directly, but it can be determined from experimental box compression strength P^*. If the box is square, it follows that $P_{fl}^* = P_{fw}^* = P^*/4l$. If the box is rectangu-

[2] McKinlay, P. Compression strength—a new insight. Unpublished. From presentation to the Forest Products Laboratory, July 1980.

[3] Note that $\sum[\log(P_{fl}/P_y) - \log(P_{fl}^*/P_y)]^2 + \sum[\log(P_{fw}/P_y) - \log(P_{fw}^*/P_y)]^2 = 2\sum(\log P - \log P^*)^2$. However, minimizing the left-hand side of the equation gives distinctly different results than minimizing the right-hand side. Properly partitioning the load-carrying capacity between the length and width panels is required to account for the observed impact of the corners on box compression strength, as described in the text.

lar, it is reasonable to iteratively proportion P^* between the side and end panels according to the ratios involving predicted box compression strength P.

$$P^*_{fl} = P_{fl}\frac{P^*}{P} = \frac{P^*/2l}{1+\frac{w}{l}\frac{P_{fw}}{P_{fl}}}$$

$$P^*_{fw} = P_{fw}\frac{P^*}{P} = \frac{P^*/2w}{1+\frac{l}{w}\frac{P_{fl}}{P_{fw}}} \quad P = 2(P_{fl}l + P_{fw}w) \tag{11}$$

We see that the side and end panels do not necessarily carry a load proportional to their fraction of the perimeter. In fact, the use of the perimeter in the original McKee Eq. (1) also runs counter to the observation in McKee et al. (1963) that the box corners apparently carry proportionally more load than do the sides. Modeling a box simply as four panels of equal impact, implicit in the use of the perimeter, misses the interaction between the panels and their failure modes that gives rise to the strengthening effects of the corners. For that reason, in solving for the panel strength of a box, we must link the deformation profiles. This extra boundary condition identifies the physics behind the extra load-carrying capacity of the corners by connecting the mode shape of the sides.

IMPLEMENTATION METHOD

Equation (9) can be expressed with either the form $y = m_1x_1 + q$ when $\tau = 0$ or the form $y = m_1x_1 + m_2x_2 + q$ when $\tau \neq 0$, and fit to data using any standard linear equation technique (for instance, the LINEST function in the Microsoft Excel spreadsheet software). Inputs y^*, x_1, and x_2 are to be computed from the expressions

$$y^* = \log\frac{P^*_{fl}}{P_y},$$

$$x_1 = u\left(\log\frac{2\hat{c}+M}{4(1-\nu^2)} + \log\frac{\overline{P_{cr}}}{P_y}\right), \text{ and}$$

$$x_2 = u\log\phi \tag{12}$$

The minimization of $\sum(y - y^*)^2$ for both side and end panels yields the outputs m_1, m_2, and q from which α, η, and τ are then computed according to

$$\alpha = 10^q,\ \eta = m_1, \text{ and } \tau = m_2/m_1 \tag{13}$$

By this technique the best fitting α, η, and τ are calculated iteratively. Initial values of P_f/P_y (Eq. (7)) yield values of P^* (Eq. (11)) and are updated iteratively until convergence.

The panel shape at failure is specified by inputting a value m that defines the number of half-waves along the panel depth. The required value of m for the weakest mode shape of the side panel is to be computed from the minimum M and lies between the integer value of ϕ denoted as ϕ_{int} and , $\phi_{int} + 1$, subject to $\phi_{int} \neq 0$. M takes on the smallest of the values

$$\phi^2 + \frac{1}{\phi^2},\ \frac{\phi^2}{\phi^2_{int}} + \frac{\phi^2_{int}}{\phi^2},\ \text{or}\ \frac{\phi^2}{\phi^2_{int}+1} + \frac{\phi^2_{int}+1}{\phi^2} \tag{14}$$

from which the required m becomes the greater of either the value 1 or the integer value of the inverse of $M(m,\phi)$ given by

$$m = \frac{\sqrt{2}\phi\sqrt{M+\sqrt{M^2-4}}}{2} \tag{15}$$

It was empirically determined by Urbanik (1996) that the same value of m found to minimize M for the finite depth side panel and used to compute P_{fl} should also be used to compute P_{fw} so as to guarantee the same mode shape in adjoining panels.

RESULTS

Meaning of α

Data with sufficient inputs to Eq. (9) were found among 17 references previously cited (see footnote (1)). The first subset of data of interest is on regular slotted corrugated containers, including SW construction from Angell and Paslay (1959), Bormett et al. (1981), Challas et al. (1994), Fahey and Bormett (1982), Frank

TABLE 2. *Results of original McKee formula applied to 29 sets of data from 17 references.*

Data set or grouping	No. samples	McKee[a] Avg |%| error	Fitted Eq. (1) a	Fitted Eq. (1) b	Fitted Eq. (1) Avg |%| error	|%| Improvement	SIE[b] α	SIE[b] η
SW boxes								
1 Angell	3	16.6	5.29	0.66	1.91	14.7	0.572	0.345
2 Bormett, Fahey, Koning	21	11.4	0.40	0.98	5.20	8.6	0.364	0.016
3 Challas	24	19.1	2.23	0.72	11.3	7.7	0.361	0.282
4 Frank waxed	78	13.2	3.74	0.65	8.42	4.7	0.400	0.347
5 Frank clamped	78	12.3	4.04	0.64	7.74	4.6	0.405	0.357
6 Gartaganis	4	16.6	0.01	1.49	6.57	10.0	0.291	−0.489
7 IPC	50	8.82	1.61	0.77	7.14	1.7	0.360	0.232
8 McKee	61	6.09	2.06	0.74	6.11	0.0	0.396	0.256
9 Schrampfer waxed	45	9.69	2.27	0.72	7.82	1.9	0.378	0.278
10 Schrampfer clamped	45	10.7	2.15	0.73	7.63	3.1	0.371	0.273
11 All SW boxes	409	11.1	2.19	0.73	9.04	2.2	0.376	0.273
12 All with *lwd*	319	11.3	2.22	0.73	9.40	2.1	0.378	0.275
DW boxes								
13 Challas	6	56.0	5.28	0.54	13.9	42.1	0.276	0.458
14 Frank waxed	4	14.5	7.36	0.58	9.4	5.1	0.475	0.425
15 Frank clamped	4	14.2	6.26	0.60	10.0	4.2	0.466	0.403
16 Schrampfer waxed	8	17.8	1.90	0.73	8.43	9.4	0.337	0.268
17 Schrampfer clamped	8	16.1	1.34	0.79	5.29	10.8	0.336	0.214
18 Shick	12	37.7	3.68	0.73	6.08	31.6	0.637	0.272
19 All DW boxes	42	31.2	3.50	0.67	28.4	2.7	0.414	0.331
SW tubes								
20 Batelka	108	41.1	3.07	0.76	11.5	29.6	0.671	0.236
21 Brodeur	15	26.7	0.42	1.02	9.35	17.3	0.479	−0.020
22 Buchanan SW	58	33.2	3.24	0.74	5.46	27.7	0.590	0.264
23 McKinlay da	8	43.4	4.81	0.71	4.94	38.5	0.721	0.294
24 McKinlay 1a	22	45.9	2.42	0.81	5.86	40.0	0.723	0.187
25 McKinlay 3c	39	44.3	1.68	0.86	10.7	33.6	0.693	0.138
26 All SW tubes	250	39.4	2.13	0.81	11.9	27.5	0.647	0.185
Other								
27 Buchanan DW	10	34.1	1.20	0.92	5.79	28.3	0.711	0.081
28 Hahn	5	22.6	6.57	0.63	7.94	14.6	0.592	0.373
29 Hartikainen	16	12.4	1.99	0.76	16.1	−3.7	0.436	0.236

[a] $a = 2.028$, $b = 0.746$.
[b] Using Eq. (9), with constraints identical to those implicitly applied by McKee: $\tau = 0$, $\nu = 0$, $\hat{c} = 1$, $u = 1$, $l = w = Z/4$, and $M = 2$.

(2004),[4] Gartaganis (1975), IPC (1967), Koning and Godshall (1975), McKee et al. (1963), and Schrampfer et al. (1987) and DW construction from Challas et al. (1994), Schrampfer et al. (1987), Shick and Chari (1965), and Frank (2004) (see also footnote 4). A second subset of data is of corrugated fiberboard tubes (boxes without top and bottom flaps) and includes SW construction from Batelka and Smith (1993), Brodeur et al. (1997), Buchanan et al. (1964), and McKinlay (see footnote 2) and DW construction from Buchanan et al. (1964). Data from tests of individual corrugated fiberboard panels by Hahn et al. (1992) and strength predictions via an alternative but not disclosed model by Hartikainen (1989) were also examined.

Twenty-nine data sets, as numbered in Table 2, were grouped and organized from the references. All references provide data on P_m, D_x, D_y, Z, and P^*. For lack of Poisson's ratio data, the assumption $\nu = 0$ was applied to all data sets. Assumption $\hat{c} = 1$ was also applied except to references from Angell and Paslay (1959),

[4] Frank, B., includes unpublished data from the Materials Testing Laboratory, Packaging Corporation of America.

Buchanan et al. (1964), and McKinlay (see footnote 2) containing data on D_{xy}, from which a more accurate $\hat{c}$ is computable. For references by Schrampfer et al. (1987) and Shick and Chari (1965) without separate l and w data and without d data, it was assumed that $l = w = Z/4$ and $M = 2$.

Data were collected by a variety of test methods; in some cases the specific method was not reported. The data from Schrampfer et al. (1987) and Frank (2004; footnote 4) are each included among "waxed" and "clamped" subsets, respectively, corresponding to the test method used to obtain P_m. For these studies, the waxed data were acquired following TAPPI T 811 (TAPPI 2002a) and the clamped data were acquired using an edge-clamping test fixture described in TAPPI T 839 (TAPPI 2002b).

The original McKee formula with constants $a = 2.028$ and $b = 0.746$ in Eq. (1) was first applied to each data set (Table 2). Little evidence exists consistent with statistical procedures for the analysis of inter-laboratory data from which it could be inferred that a and b are actually constant. Nevertheless, Batelka and Smith (1993), Brodeur et al. (1997), Challas et al. (1994), IPC (1967), and Schrampfer et al. (1987) advocated applying the "McKee constants" to their data.

The average absolute values of the difference between actual and predicted results from fitting each of the 29 data groupings independently to the form of Eq. (1) with the standard McKee constants are given in Table 2. We found much higher average differences in many of the data sets than those reported in McKee et al. (1963). By letting a and b vary independently for each data set, we could improve the individual fits. The typical improvement in the average magnitude of the percent error of a data set is 5.7% for SW box data sets 1–10, 17.2% for DW box data sets 13–18, and 31.1% for SW tube data sets 20–25. However, the resulting a and b values then differ significantly, both from those presented by McKee and across the range of different data sets. The average error magnitudes of the predictions using the McKee values would necessitate an impractical safety factor, and the individually fitted values for a and b vary widely; therefore, there appears to be little justification for assuming that a and b are truly constant.

When we apply the same constraints to Eq. (9) as applied in McKee et al. (1963) and discussed previously, the α and η values are simply transformations of the a and b values (Table 2). The predicted panel strength ratio P_f/P_y determined for data set 3 from Challas et al. (1994) is compared with the respective experimental panel strength ratio P_f^*/P_y as the strength ratios vary with slenderness U in Fig. 1. In this first analysis, the critical load given by $\overline{P_{cr}}$ is used to compute U. The physical significance of α and η is identified on the plot. These first results are coded S I E to designate square (S), infinite depth (I), and elastic (E) buckling constraints. Later we will examine modifications to these constraints, including rectangular (R) and finite depth (F) boxes with a combination elastic–inelastic (EI) buckling constraint.

The differences between evaluations in terms of a or α are noteworthy. Except for data set 1 from Angell and Paslay (1959) with only three samples, the α-levels determined for SW boxes are consistently lower than those determined for SW tubes (Table 2). Examining the confidence

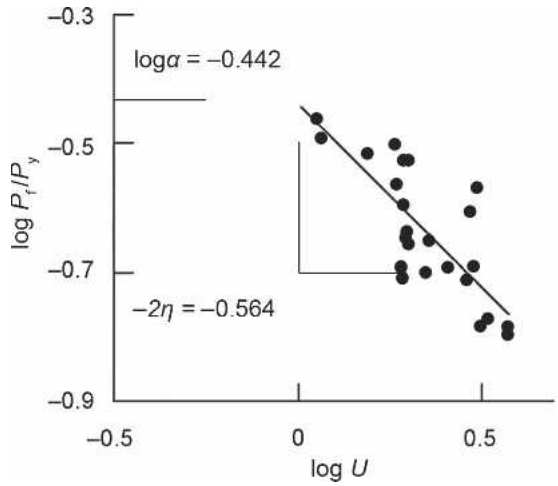

FIG. 1. Plot of Eq. (9) with $u = 1$ for all panels fit to data set 3 from Challas et al. (1994) (Table II), characterized by Eq. (11) and shown in relation to universal slenderness U of box panels. Fit is determined for model S I E, as explained in text.

intervals (Fig. 2), we see that nearly all the α–values for the SW boxes are similar and generally do not overlap with those for the tubes (with the exception of the small data set of tubes from Broduer et al. (1997)). A similar contrast in terms of *a*-levels is not apparent.

The prefactor (α or *a*) gives the function its scale. We now see one of the advantages of writing the equation in terms of α and η, as in Eq. (7), instead of *a* and *b*, as in Eq. (8). As noted in the introduction, reported values for *a* vary broadly in the literature, effectively changing the estimate for box compression significantly. If we examine only the SW box data sets with more than 20 samples, the best fitting *a* still spans an order of magnitude ranging from 0.4 to 4.0. The overall range in *a* is even larger. That appears to imply a significant spread in the estimate of box compression strength, though in actuality the corresponding adjustments to *b* tighten the range. Essentially, the use of *a*-values removes any physical meaning from the prefactor beyond simply being a fitted parameter. By contrast, the α-values for the same SW box data sets have confidence intervals (Fig. 2) that nearly all overlap and are distinctly different from the values for tubes.

Tube compression strength is higher than box compression strength for similar materials cut to the same size and shape. We find an explanation for increased strength in α that is missing when we look only at *a* values. From a compression perspective, the difference between tubes and boxes lies only in the presence of a score-line and flap at the loading point. Thus, the drop in the fitted α-level from tubes to boxes is a physical quantification of the strength around the horizontal loading edge as it is impacted by the scoring. This strength is relative to the experimental edgewise crush strength, with the different α-levels (the scale factor in the box estimation) reflecting the fact that boxes are inherently weaker than tubes because of flap scores.

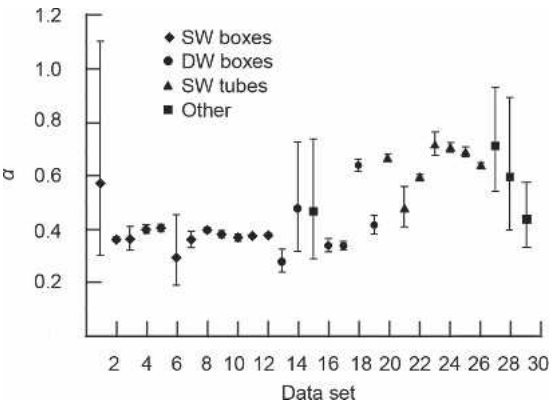

FIG. 2. Approximate 95% confidence intervals determined for α calculated from exact confidence intervals determined for log α in Eq. (9) using S E I constraints. Data sets 11, 12, 19, and 26 are data groupings as described in the text and are not independent of other sets in their groups.

We believe our results in Fig. 2 are the first identification of a parameter relating score-line mechanics to box compressive strength. In early experiments, Carlson (1941) examined the shape of the box load–compression curve in relation to scoring depth and found that deeper scoring yielded greater compression at a given load. Work through the Fourdrinier Kraft Board Institute (1953) explored the loss of compression strength that occurs with scoring. Urbanik (1990) quantified the spring rate of scored edges in relation to the vibration response of stacked containers and determined that scored edges stiffen with increasing load. Collectively, parameter α appears to be a complicated function of fabrication, geometry, experimental methods, and modeling assumptions.

With both *a* and α values, the prefactor for DW boxes ranges widely (Fig. 2). In some data sets the DW model appears similar to SW boxes, whereas in others it appears similar to tubes. In nearly all the individual data sets, the number of data points is small and the data are unevenly distributed across the design space. In roughly half the data, we also must make assumptions about box dimensions. Despite these limitations, the α-values are essentially bounded by the values for tubes and those for boxes. Understanding the tube values to describe the limiting case when the score profile does not impact the box compression strength and box values to describe the range of impact from typical scoring, we might expect this breadth in results. Scoring can affect DW boxes in a variety of ways, given the

larger range of score depth and profile possible on a DW box. This impact may account for why some DW data sets significantly outperform the typical (McKee) estimation for compression strength while others significantly underperform the same estimation. Unfortunately, since the data are limited and the scoring method and type are not reported for any of the data sets in the literature, this hypothesis cannot be pursued further.

Removing constraints

The preceding analysis examined fitting Eq. (9) while maintaining the constraints applied by McKee et al. (1963). In general, we want to find the model where the prediction error between P and P^* is minimized, in practice by finding the α and η values that minimize Eq. (10). Sixteen models of Eq. (9), with each combination of the four constraints retained or removed as discussed in the previous text, were fit to each data set as appropriate. The average error magnitudes for the best fitting model in comparison with model S I E are given in Fig. 3 for each SW box data set and in Fig. 4 for the remaining data sets. As noted, these models are coded for assumptions/constraints of square (S) or rectangular (R) geometry, infinite (I) or finite (F) depth, and elastic (E) or combined elastic–inelastic (EI) buckling, as well as whether or not they incorporate the empirical factor τ.

As mentioned previously, all these models are totally consistent with the underlying theory of McKee et al. (1963) but have different constraints. Results of applying models with $\tau \neq 0$ are shown in Figs. 3 and 4 as well. Not all data sets can be modeled with all the constraints removed. The Angell and Paslay (1959) data, with only three points, becomes under-constrained when we add τ to the model. Since the Shick and Chari (1965) and Schrampfer et al. (1987) data sets do not include explicit box dimensions, we assume square, infinitely deep boxes for these

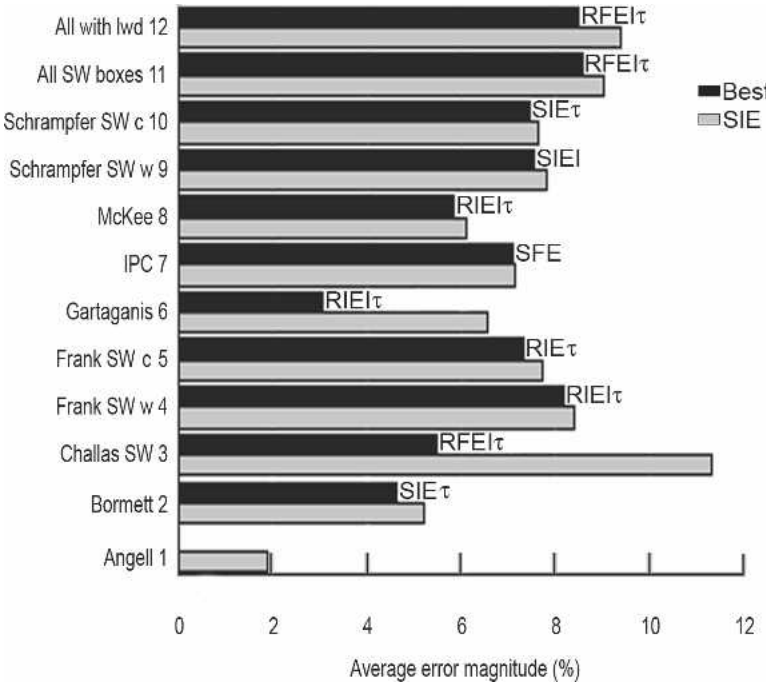

FIG. 3. Average error magnitudes between P and P^* determined for best (Best) of 16 models applied to SW box data sets in Table 2 compared with average error magnitude for model S I E (SIE). SW, single-wall; c, clamped; w, waxed; lwd, length, width, depth.

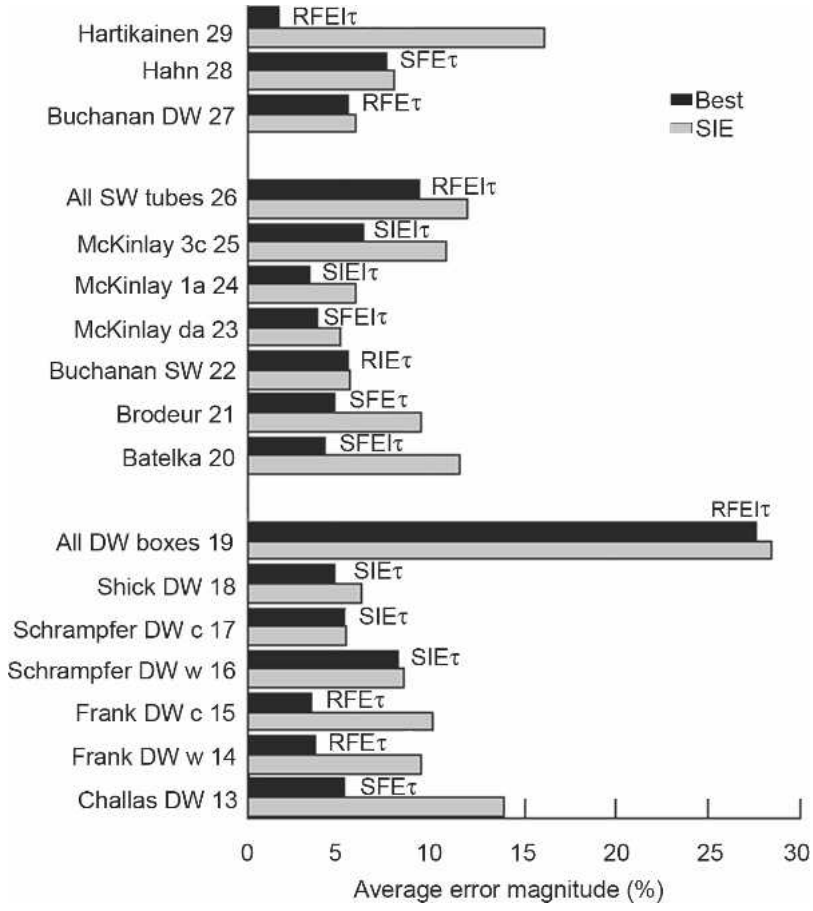

FIG. 4. Average error magnitudes between P and P^* determined for best (Best) of 16 models applied to DW box, tube, and other data sets in Table 2 compared with average error magnitude for model S I E (SIE). Legends explained in text. DW, double-wall.

data sets in the initial analysis and do not analyze them with other models.

The improvement in the accuracy of our models as we relax various constraints is clear for most of the data sets (Figs. 3, 4), though the specific model that fits each data set best depends on the data set itself. Experiments by Challas et al. (1994) and Frank (2004; footnote 4) were in whole or in part explicitly designed to test the effects of box geometry beyond the McKee constraints, whereas experiments in IPC (1967) specifically avoided one or more constraints.

An example plot of predicted and experimental strength ratios from model R F EI applied to data set 3 from Challas et al. (1994) is shown in Fig. 5. For this case and for all EI models, slenderness, the square root of the ratio of the yield strength to the critical load, is to be calculated from the critical load given by

$$P_{cr} = \phi^{\tau} \frac{2\hat{c} + M}{4(1 - \nu^2)} \overline{P_{cr}} \tag{16}$$

Then if U of a panel is computed to be greater than 1, u in Eq. (9) is assigned a value of 1. Otherwise, u is assigned a value of 0. In contrast with Fig. 1, Fig. 5 differentiates between elastic and inelastic modes of failure and reveals a difference between side panel and end panel performance. The calculated level of α (Fig. 5) is the maximum strength per loading edge determined for the scoring geometry applied.

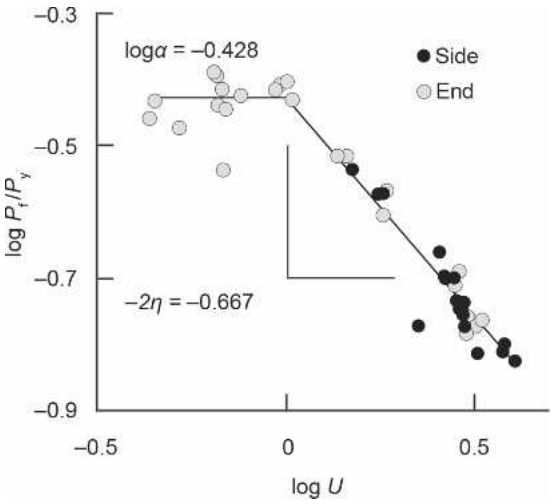

FIG. 5. Plot of Eq. (9) fit to data set 3 from Challas et al. (1994) (Table 2), characterized by Eq. (11) and shown in relation to universal slenderness U of box panels. Fit is determined for model R F EI as explained in text. In contrast with Fig. 1, u in Eq. (9) is assigned a value of 0 or 1 depending on level of U computed for each panel.

In model S I E and model R F EI, for example, it was assumed that $\tau = 0$. An implicit law in the simplified calculation of P_{cr} is that the buckled wave shape is symmetric and the stress distribution up to buckling remains uniform. However, more sophisticated calculations in Urbanik and Saliklis (2003) led to weaker nonsymmetrical patterns. Parameter τ empirically corrects the determination of ϕ for input to P_{cr}. Results of applying models with $\tau \neq 0$ are considered in generating Figs. 3 and 4. In some cases the best fit model does not incorporate τ, and results with $\tau = 0$ are considered as well.

The significance of including parameter τ in Eq. (9) was quantified by applying the statistical F-distribution to the sum of errors squared from Eq. (9) with $\tau = 0$, and the sum of errors squared with $\tau \neq 0$. Consistent with Urbanik and Saliklis (2003), including τ as a third parameter along with α and η was determined to be statistically significant for many of the individual models. A global model including τ was thus sought. Other evidence in an analysis by Urbanik (1996) of some tube literature suggests that a nonlinear material law further increases model accuracy. Since τ is a correction made in part to account for nonsymmetrical failure, it may not be possible to totally determine the physical significance of τ using only a linear material law. The results of this work based on a linear material law can provide the input to other models based on a nonlinear material law.

Toward a global SW model

The various α values (Fig. 2) and the previous discussion clearly indicate that it is not appropriate to try to model box compression results using data from structures that are not boxes. Further, the range in values for the fitting parameters for DW boxes and considerations of asymmetry evident in Libove and Hubka (1951) indicate that variation across data sets and perhaps a variable associated with the scoring profile are not accounted for in the available data. Thus, our focus for further analysis must shift to the available data on SW boxes.

Since our goal in developing a predictive model is not to form a large subset of models each describing individual data sets under various constraints but rather to generate a single model that can be applied broadly, we need to examine different approaches to unifying the data. One method is to group all the data sets together and analyze them statistically using blocking techniques, where each data set forms its own block. This statistical technique assumes that each data set might have its own offset due to differences in measurement method, equipment, and other variables. It then calculates and removes these potential sources of variation from the analysis before the effects of the independent variables of interest are tested for significance against the noise. When we do this for a given set of constraints, we generate a "universal" α and η along with a set of offsets for each data set. However, without incorporating those offsets into the calculation explicitly, the standard error of the resulting model applied to each data set individually and the resulting uncertainty and error in a given prediction are higher than that for a general model without blocking. In general, it would not be practical, even if possible, to calculate an offset value for

every laboratory before performing an estimation of box compression strength. Thus, the blocking approach, while mathematically robust, does not enhance our ability to estimate general box performance.

We would hope that the offsets calculated in the blocking process would at least reveal additional information about differences in parameter testing method. For instance, if one ECT method consistently led to stronger or more robust estimations of box performance, we would believe that it was a better measure of the inherent strength of the combined board. However, the results are not uniform across the available data sets; while α and η values are higher for the Frank (2004; footnote 4) data when comparing the clamp to the waxed ECT, the converse is true for the Schrampfer et al. (1987) data. (Trends are more consistent for the DW results, but the data are too sparse to draw robust conclusions.) Additional work in this area may help clarify which of the various ECT methods in use in the field best models box performance and may similarly shed light on other differences in testing technique.

Analyzing all the SW data as a single unified group without blocking allows us to generate a model encompassing all the data. The advantage of this approach is that our model becomes general, explicitly incorporating between-lab sources of testing variability. Thus, it should apply equally well to any additional (future, or existing and unpublished) data sets from other sources. However, it is important to keep in mind the constraints on each individual data set since not all sources include all the parameters for a full fit to the model. We can use all the SW data sets when applying the S I E model, as discussed earlier. However, when we switch to rectangular (R) or finite (F) constraints, we must leave out the data points from Schrampfer et al. (1987) since that reference does not explicitly include dimensional information on the boxes tested, and we would have to assume the boxes were square and infinite even in a fitting routine with R or F constraints. This would be expected to inappropriately bias the fitting results. By including all the available data independent of the method used to measure P_m, we lose any ability to further explore the impact of different measurement methods.

The 16 resultant models with different combinations of constraints applied to our large SW box data set appear in Table 3. We find that on average and neglecting interactions, relaxing the constraint that all the boxes are square improves our typical absolute value of the error by 0.07%; relaxing the constraint on the depth of the box improves our estimate by 0.18% on average; including inelastic failure as a possibility in the model improves our estimate by 0.34% on average; and including τ improves the estimate by 0.12% on average. The model with the lowest average error in estimated box strength is the one where all these terms are included. We also see that models that relax more than one constraint typically improve the average error by more than the sum of the individual improvements. This is a clear indication of interaction terms in the factorial analysis. We would expect these interactions given that (for example) removing the constraint that all boxes are infinitely deep allows additional data points to fall into the elastic–inelastic regime. The best fitting model is the one in which all the constraints are removed (R F EIτ).

SW model variability

A measure of the economic practicality of our SW model is given in Table 4 and Fig. 6. Table 4 presents the mean and standard deviation, assuming a normal distribution, of the percent prediction errors $P - P^*$ for some selected models. Analysis of the round-robin data in Miles (1966), following procedures in ASTM E 691 (ASTM 1999), yields a between-laboratory reproducibility standard deviation of 7.74%. Analysis for ASTM D 642 (ASTM 2003) recommends a between-laboratory reproducibility of 11.3%,[5] with subsequent retesting and analy-

[5] The reproducibility standard deviation can be determined from $11.3\%/1.96\sqrt{2} = 4.08\%$ (ASTM E 691). Thus, no model based on historical data can be expected to have a standard deviation less than 4.08% (as distinct from any systematic bias), even after extensive testing and retesting.

TABLE 3. *Results from fitting all SW box data as a uniform data set for 16 different models incorporating different constraints.*[a]

Data	Model with constraints	α	η	τ	Avg. |%| error	r^2
All SW data	S I E	0.376	0.273	0	9.04	0.911
	S I E τ	0.377	0.274	−0.007	9.04	0.911
	S I EI	0.387	0.295	0	8.87	0.914
	S I EI τ	0.389	0.297	−0.020	8.86	0.914
All SW data with *lwd* dimensions	S I E	0.378	0.275	0	9.40	0.912
	S F E	0.376	0.282	0	9.14	0.911
	R I E	0.378	0.271	0	9.25	0.914
	R F E	0.365	0.262	0	9.44	0.904
	S I E τ	0.376	0.272	0.091	9.35	0.913
	S F E τ	0.372	0.277	0.289	8.96	0.921
	R I E τ	0.377	0.269	0.065	9.22	0.915
	R F E τ	0.362	0.257	0.202	9.30	0.911
	S I EI	0.387	0.293	0	9.18	0.916
	S F EI	0.386	0.302	0	8.94	0.915
	R I EI	0.395	0.300	0	8.95	0.918
	R F EI	0.390	0.310	0	8.87	0.914
	S I EI τ	0.387	0.292	0.035	9.17	0.916
	S F EI τ	0.384	0.300	0.262	8.83	0.925
	R I EI τ	0.394	0.298	0.080	8.90	0.920
	R F EI τ	0.391	0.312	0.359	8.47	0.930

[a] Data from Schrampfer et al. (1987) are only included among S and I models.

TABLE 4. *Mean and standard deviation of prediction errors between P and P* determined for selected models.*[a]

Model and data	Avg. |%| error	Mean (%)	Standard deviation (%)
Miles inter-laboratory data reproducibility	—	0.00	7.74
McKee formula with McKee data	6.09	0.29	7.75
McKee formula with all SW data	11.1	7.64	11.9
S I E model with all SW data	8.99	0.62	11.1
R F EI τ model with all SW data with *lwd* dimensions	8.48	0.56	10.6

[a] Average error includes both the accuracy of fit to specific data set and any systematic bias in data. Mean error is a measure of systematic bias in fit. The mean of Miles data is taken to be zero by definition because it is simply the mean of all identical boxes measured in this study. Standard deviation indicates variability of data set about the mean. For a perfect distribution, average error should occur at 0.675 times the standard deviation. In all cases, our average error is higher, indicating a higher fraction of the population in the "wings" of the distribution than would be expected in a truly "normal" distribution.

sis reducing the inter-laboratory variation to 4.08%.[5] But such intense retesting is too costly to advocate for typical production control. The Miles (1966) variation provides an objective measure of how good any model can be expected to be. Current inter-laboratory round-robin studies from Collaborative Testing Services (2004) show similar levels of variability when a uniform method of sealing boxes is considered. Figure 6 shows the normalized frequency distribution fit to the prediction errors.

Variation statistics of various model and data combinations are also given in Table 4. The means of the prediction errors of the fitted models are not exactly zero because Eq. (10) is being minimized in the fit instead of the absolute value of the error, $\sum(P - P^*)^2$. Interestingly, the variation of the original McKee formula fit to the McKee et al. (1963) data is almost identical to the Miles (1966) variation (Table 4). However, when the McKee formula is fit to other available SW data, variation increases to 11.9% (Table 4). When we model all the data with McKee, we also find that the mean of the prediction errors is greater than zero (Fig. 6). This implies that McKee consistently overpredicts the measured box strength in the larger data set by nearly

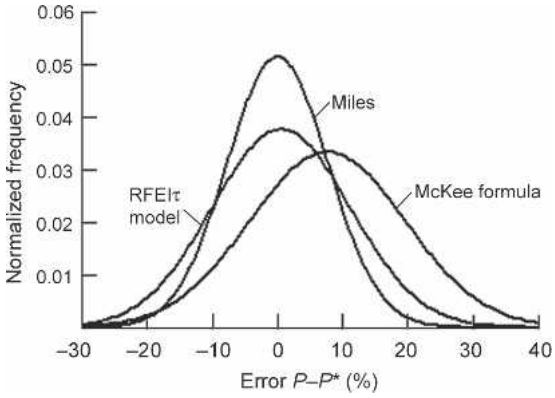

FIG. 6. Frequency distribution, normalized to have areas equal to 1, for three model and data combinations from Table 4. Legends refer to Miles inter-laboratory data reproducibility, McKee formula with all SW data, and R F EI τ model with all SW data with *lwd* dimensions (Table 4).

7.5%, on top of the large variation (standard deviation) in the prediction.

The available SW data are most accurately quantified (mean closest to zero and lowest percentage of error magnitude) (Table 4) with the R F EI τ model (Fig. 6) with all constraints removed. The difference in standard deviation between the R F EI τ model and the Miles (1966) data is a measure of further improvements to expect from including twisting mechanical properties, score-line properties, and explicit nonlinear behavior in the model.

We can most easily quantify the advantage of the improvement in model precision using a model box. The accuracy of each model explored is defined by the average magnitude of the % error (|%| error), listed in Tables 3 and 4 for each of the models explored. If we assume a box with a "true" compression strength of 1000 lbs (453 kg), the Miles data indicate that in testing we might find values from 923 to 1077 lbs (418 to 488 kg) at 1-sigma. The McKee estimate would fall in the range of 968 to 1195 lbs, (439 to 542 kg) with an average estimate of 1076 lbs (488 kg). On average, the McKee estimate would be 7.64% high, and as we can see, even within a 1-sigma range of uncertainty, it might be as much as 19% high. This uncertainty in the accuracy of the estimate leads to high "safety factors" on box design out of necessity, as discussed in the above. By contrast, the R F EI τ model would fall in the range of 922 to 1091 lbs (418 to 494 kg), with an average estimate of 1006 lbs (456 kg). Thus, the improved model prediction is much closer to the average range we would find in testing the actual box at a variety of testing labs.

It would be interesting to compare our model to an independent data set to quantify the improvement gained by the model. However, all the available robust sets where data are sufficiently described to be able to apply the model were included in generating model parameters. As observed for most cases in Figs. 3 and 4, the average estimation error is reduced for each of these data sets when one or more of the constraints assumed by McKee et al. (1963) are removed. Thus, to quantify the fit we must choose other independent data sets that may have problems with input parameters. The joint confidence region for fitted parameters α and η in our R F EI τ model is shown in Fig. 7 as well as joint confidence regions for two other data sets. The joint confidence region for the R F EI τ model fit to data from Little (1943)[6] is significantly different than that of our SW model.

The edge-crush data in Little (1943) were affected by stress concentrations in a notched test specimen, which consequently inflates the fitted α. Data in Koning and Moody (1969) include intentionally defective edge-crush specimens tested by TAPPI T811 (TAPPI 2002a). Our SW fit matches the Koning and Moody (1969) box strength data with an average error magnitude of 4.8%. But, more significantly, the joint confidence region for the R F EI τ model fit to the Koning and Moody (1969) data is sweepingly large. As shown in Fig. 7, differences in the joint confidence regions representing our model and other data sets can reveal poor test methods, albeit with low variability, or high parameter variability resulting from high material variability sensed by a correct test method.

[6] D_x data are not given in Little (1943) and $D_x/D_y = 2$ was assumed to apply.

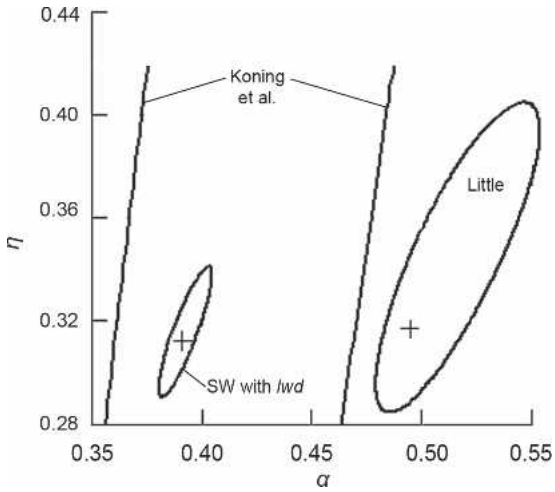

FIG. 7. 95% joint confidence regions for parameters α and η determined for R F EI τ model with $\tau = 0.36$ and fit to all SW data with *lwd* dimensions, data from Little (1943), and data from Koning and Moody. (1969). Only a section of the Koning and Moody (1969) confidence region is shown plotted.

CONCLUSIONS

Until recently, the state of the art of box compression estimation was the equation by McKee et al. (1963) or various modifications, with the assumption that Eq. (1) provided an estimation that was accurate to within about 6% on average and 15% for the majority of single-wall boxes. In reality, we see that for a broader data set of single-wall boxes, the McKee equation systematically overestimates compression strength. It provides an estimate within about 11% of the true box compression value on average, and the strength estimates of many boxes are off by more than 20%. The estimated strength of double-wall boxes and tube constructions can be off by even more.

By applying the results and approach of Urbanik and Saliklis (2003) to the available data sets in the literature, we gained a deeper understanding of the differences in performance among box structures, as well as refined the precision of our estimations. By removing the constraints and assumptions in the McKee equation, which were necessary in 1963 because of limitations in computing tools, we improved our estimation for single-wall boxes to ±8.5% on average. The resulting 10.6% standard deviation among the prediction errors compares with about 7.7% attainable through inter-laboratory testing and is a measure of modeling variation given available data. Our model allows for additional inputs related to combined board twisting mechanics and to score-line properties if such broadened data can be obtained.

Further, we can now attach physical meaning to what were previously only fitting parameters. We see that not only does the prefactor α give the function its scale, it also relates to the strength around the score of the box. This explains why single-wall, double-wall, and tube constructions are not modeled with equal accuracy by Eq. (1) and highlights some additional information that would be necessary to create such models. The exponent η explicitly relates the relative impact of the contributions from bending stiffness, panel size, and inherent material compressive strength. While this is the same function as that of the exponent in Eq. (1), writing the expression in terms of α and η instead of a and b disentangles the function scale factor from the relative proportioning of the contributions from the box material parameters. Finally, parameter τ helps us correct for the assumption that the box is failing symmetrically. This assumption is obviously violated in most real-world box failures, but it is required in the application of a closed form calculation of P_{cr}.

Overall, this approach allows the improvement of package construction to better meet customer requirements and provides more objective criteria to establish safety factors. It also provides a tool for additional explorations in box optimization, from score profile optimization to the selection of the ECT method that best correlates to actual box performance. Further work exploring the application of a nonlinear material law to box failure may shed additional light on these and other issues.

NOMENCLATURE

a, b = McKee formula constants
C = Linear material law parameter derived in Johnson and Urbanik (1987)

$\hat{c}$ = Normalized in-plane shear modulus of elasticity derived in Urbanik (1992) and computable by $\hat{c} = v + 2(1 - v^2)(D_{xy}/D_x)\sqrt{D_y/D_x}$ for corrugated fiberboard

D_x, D_y, D_{xy} = Flexural stiffness per unit width in transverse, axial, and twisting directions

d = Plate length equal to box depth

l, w = Plate width equal to box length, box width. As subscripts, box side panel, end panel

M = Mode shape function

m = Number of buckled half-waves

m_1, m_2, q = Spreadsheet constants

P, P^* = Box compression strength (predicted, experimental)

P_{cr} = Plate critical load per unit width

$\overline{P_{cr}}$ = Value of P_{cr} for infinite length plate when $v = 0$ and $\hat{c} = 1$ and given by $\overline{P_{cr}} = (4\pi^2\sqrt{D_xD_y}/l^2)$

P_1 = Plate strength

P_m = Edgewise crush strength per unit width

P_y = Plate yield strength per unit width. For corrugated fiberboard $P_y = P_m$

P_f, P_f^* = Plate strength per unit width (predicted, experimental)

S = Dimensionless plate stiffness given by $S = (12\sqrt{D_xD_y}/\theta_0P_yl^2)$

U = Universal slenderness given by $U = \sqrt{P_y/P_{cr}}$

u = Elastic–inelastic criterion

x_1, x_2, y, y^* = Spreadsheet variables

Z = Box perimeter

α, η = Postbuckling constants

ϕ = Effective plate aspect ratio given by $\phi = (d/l)(D_x/D_y)^{1/4}$

ϕ_{int} = Integer component of ϕ

θ_0 = Stress–strain curvature

$\hat{\sigma}_a$ = Apparent dimensionless buckling stress

τ = Empirical improvement

v = Geometric mean Poisson's ratio

χ = Wave length

REFERENCES

ANGELL, B. S., AND P. R. PASLAY. 1959. Prediction of short-time static compressive strength of corrugated containers. Tappi J. 42(6):194A–199A.

AMERICAN SOCIETY FOR TESTING AND MATERIALS (ASTM). 1999. Standard practice for conducting an interlaboratory study to determine the precision of a test method. ASTM E 691. American Society for Testing and Materials, West Conshohocken, PA.

———, 2003. Standard test method for determining compressive resistance of shipping containers, components, and unit loads. ASTM D 642. American Society for Testing and Materials, West Conshohocken, PA.

BATELKA, J. J., AND C. N. SMITH. 1993. Package compression model. IPST Project 3746, final report. Institute of Paper Science and Technology, Georgia Institute of Technology, Atlanta, GA.

BORMETT, D. W., D. J. FAHEY, AND J. F. LAUNDRIE. 1981. Use of oak in linerboard. Res. Pap. RP–FPL–410. USDA, Forest Serv., Forest Prod. Lab., Madison, WI.

BRODEUR, P. H., I. M. HUTTEN, AND J. L. JONAKIN. 1997. MD and CD properties of linerboard components and the resulting box compressive strength. Tappi J. 80(10):27–35.

BUCHANAN, J. S., J. DRAPER, AND G. W. TEAGUE. 1964. Combined board characteristics that determine box performance. Paperboard Packaging, September:74–85.

CARLSON, T. A. 1941. Factors affecting the compressive strength of fibre boxes. Fibre Containers 26(3):28–35.

CHALLAS, J., M. SCHAEPE, AND C. N. SMITH. 1994. Predicting package compression strength geometry effect. IPST Project 3806, final report. Institute of Paper Science and Technology, Georgia Institute of Technology, Atlanta, GA.

COLLABORATIVE TESTING SERVICES. 2004. Analysis 301, reports for cycles 201, 203, 205, 207, 209, 211, and 213. Collaborative Testing Services, Inc., Sterling, VA. http://www.collaborativetesting.com/paper/current_report.html

FAHEY, D. J., AND D. W. BORMETT. 1982. Recycled fibers in corrugated fiberboard containers. Tappi J. 65(10):107–110.

FOURDRINIER KRAFT BOARD INSTITUTE. 1953. Testing compression reports 39 and 41. Institute of Paper Chemistry, Appleton, WI.

FRANK, B. 2004. Caliper or weighted caliper for evaluating boxes. Corrugating International, October:3–8.

GARTAGANIS, P. A. 1975. Strength properties of corrugated containers. Tappi J. 58(11).

HAHN, E. K., A. DE RUVO, B. S. WESTERLIND, AND L. A. CARLSSON. 1992. Compressive strength of edge-loaded corrugated board panels. Exper. Mech., September:259–265.

HARTIKAINEN, K. 1989. CAB—Computer aided box optimization, F.E.F.C.O. *In* Proc. 5th FEFCO Technical Seminar, Nice, France.

IPC. 1967. The effect of distribution of stiffness between components on the compressive performance of corru-

gated boxes. Testing compression report 85, Project 2695–3. Institute of Paper Chemistry. Appleton, WI: Pp. 1–52.

JOHNSON, M. J., JR., AND T. J. URBANIK. 1987. Buckling of axially loaded, long rectangular paperboard plates. Wood Fiber Sci. 19(2):135–146.

KAWABATA, Y. 1997. New calculating method for compression strength of corrugated linerboard box—Concentrated on new Kellicutt equation. J. Korea Tappi 29(4):73–85.

KELLICUT, K. Q., AND E. F. LANDT. 1951. Basic design data for use of fiberboard in shipping containers. Fibre Containers 36(12):62–80.

KONING, J. W., JR., AND R. C. MOODY. 1969. Effect of glue skips on compressive strength of corrugated fiberboard containers. Tappi J. 52(10):1910–1915.

———, AND W. D. GODSHALL. 1975. Repeated recycling of corrugated containers and its effect on strength properties. Tappi J. 58(9):146–150.

LIBOVE, C. L., AND R. E. HUBKA. 1951. Elastic constants for corrugated-core sandwich plates. National Advisory Committee for Aeronautics, Tech. Note 2289. NASA Center for Aerospace, Hanover, MD.

LITTLE, J. R. 1943. A theory of box compressive resistance in relation to the structural properties of corrugated paperboard. Paper Trade J. 116(24):31–34.

LUO, S., J. C. SUHLING, AND T. L. LAUFENBERG. 1995. Bending and twisting tests for measurement of the stiffnesses of corrugated board. AMD-Vol. 209/MD Vol. 60, Mechan. Cellulosic Mat. ASME: 91–109.

MCKEE, R. C., J. W. GANDER, AND J. R. WACHUTA. 1963. Compression strength formula for corrugated boxes, Paperboard Packaging, August, 149–159.

MCKINLAY, P. 1980. See footnote no. 2.

MILES, J. G. 1966. Compressive strength of corrugated containers: An interlaboratory study. Mater. Res. Standards, March:142–146.

SCHRAMPFER, K. E., W. J. WHITSITT, AND G. A. BAUM. 1987. Combined board edge crush technology. IPC Project 2695–24 Progress Report 1. Institute of Paper Chemistry, Appleton, WI.

SHICK, P. E., AND N. C. S. CHARI. 1965. Top-to-bottom compression for double wall corrugated boxes. Tappi J. 48(7): 423–430.

TAPPI. 2002a. Edgewise compressive strength of corrugated fiberboard. (Short column test).Tappi T811 om 02. TAPPI, Norcross, GA.

———, 2002b. Edgewise compressive strength of corrugated fiberboard using the clamp method. (Short column test). Tappi T839 om 02. TAPPI, Norcross, GA.

URBANIK, T. J. 1990. Forced vibration response of nonlinear top-loaded corrugated fiberboard containers. Pages 253–274, Vol. 1 *In* Proc., 61st Shock and Vibration Symposium, Pasadena, CA.

———, 1992. Effect of in-plane shear modulus of elasticity on buckling strength of paperboard plates. Wood Fiber Sci. 24(4):381–384.

———, 1996. Review of buckling mode and geometry effects on postbuckling strength of corrugated containers. PVP–Vol. 343, Development, validation, and application of inelastic methods for structural analysis and design, ASME, pp. 85–94.

———, AND E. P. SALIKLIS. 2003. Finite element corroboration of buckling phenomena observed in corrugated boxes. Wood Fiber Sci. 35(3):322–333.

WOLF, M. 1972. New equation helps pin down box specifications. Package Engineering, March:66–67.